Glutamate release by primary brain tumors induces epileptic activity

Susan C Buckingham, Susan L Campbell, Brian R Haas, Vedrana Montana, Stefanie Robel, Toyin Ogunrinu & Harald Sontheimer

Epileptic seizures are a common and poorly understood comorbidity for individuals with primary brain tumors. To investigate peritumoral seizure etiology, we implanted human-derived glioma cells into severe combined immunodeficient mice. Within 14–18 d, glioma-bearing mice developed spontaneous and recurring abnormal electroencephalogram events consistent with progressive epileptic activity. Acute brain slices from these mice showed marked glutamate release from the tumor mediated by the system x_c^- cystine-glutamate transporter (encoded by *Slc7a11*). Biophysical and optical recordings showed glutamatergic epileptiform hyperexcitability that spread into adjacent brain tissue. We inhibited glutamate release from the tumor and the ensuing hyperexcitability by sulfasalazine (SAS), a US Food and Drug Administration–approved drug that blocks system x_c^-. We found that acute administration of SAS at concentrations equivalent to those used to treat Crohn's disease in humans reduced epileptic event frequency in tumor-bearing mice compared with untreated controls. SAS should be considered as an adjuvant treatment to ameliorate peritumoral seizures associated with glioma in humans.

Gliomas are the deadliest and most common of primary brain tumors, and they currently lack effective treatments. They grow relentlessly, often causing profound neurological impairments as the enlarging tumor impinges on vital brain structures. Peritumoral seizures are an early symptom and up to 80% of individuals with glioma experience at least one seizure during the course of their illness[1,2]. Approximately one-third of individuals develop recurrent seizures, known as tumor-associated epilepsy[3], and these can be refractory to traditional antiepileptic medication[2]. The etiology of tumor-associated seizures and their relationship with tumor growth is poorly understood. Increased glutamate levels have been implicated in numerous seizure disorders, and glutamate can reach neurotoxic levels immediately preceding and during spontaneous seizures[4]. Previous studies conducted in both humans with glioma and glioma-implanted rodents have suggested that epileptiform activity originates within the peritumoral border, 1-2 mm away from the tumor mass, where invading tumor cells surround neurons[5–7]. A recent clinical study involving nine glioma patients examined glutamate concentrations in central nervous system dialysates taken from peritumoral cortex and from uninvolved brain, and found peritumoral glutamate concentrations above 100 µM, 100-fold higher than levels in uninvolved brain[8]. This increase in peritumoral glutamate may be ascribed to the activity of system x_c^-, a Na^+-independent cystine-glutamate transporter[9–11]. System x_c^- is a heterodimeric transporter consisting of a catalytic (xCT) and a regulatory (CD98) subunit, both of which are highly expressed by glioma cells[12]. System x_c^- imports cystine for the synthesis of the antioxidant glutathione, and cystine uptake is coupled to glutamate release[13,14].

In this study, we hypothesize that glutamate release from gliomas through system x_c^- activates glutamate receptors on peritumoral neurons, leading to neuronal hyperexcitability and epileptic activity. To elucidate the possible relationship between tumor-mediated glutamate release and epileptic activity, we modeled the disease in glioma-bearing mice to permit both *in vivo* and *in situ* analysis. Using electroencephalogram (EEG) recordings, we found that abnormal EEG activity develops in tumor-bearing mice but not in controls. This activity presents as short-duration abnormal EEG events that typically increase in frequency as the tumor progresses. Brain slices prepared from these mice show enhanced glutamate release and peritumoral neuronal hyperexcitability. This excitability spreads into the tumor-associated brain, as shown by optical recordings. Notably, pharmacological inhibition of system x_c^-–mediated glutamate release from gliomas by SAS, a US Food and Drug Administration (FDA)-approved drug, inhibits peritumoral hyperexcitability and reduces epileptic event frequency in tumor-bearing mice.

RESULTS

Glioma-bearing mice show recurrent epileptic activity

We adopted a widely used mouse model of glioma[15,16] to study the relationship between glutamate release from glioma cells and the development of epileptic activity *in vivo*. Specifically, we implanted either the U251-GFP human glioma cell line or the human glioma xenografts GBM12 and GBM22 intracranially into mice. The glioma xenografts originated from two patient biopsies and were propagated by ectopic implantation into the flanks of nude mice[17]. These xenografts are currently considered the best available glioma model

Figure 1 Tumor-bearing mice show abnormal spontaneous EEG events indicative of epileptic activity. (**a**) Representative EEG recordings from three glioma-implanted mice, juxtaposing abnormal events and baselines for each. (**b**) A power spectrum from one representative event (inset) and the corresponding baseline from the same mouse. (**c**) Frequency of epileptic activity in 13 tumor-bearing mice quantified over 10 consecutive d; hourly event frequency is plotted as a function of time. (**d**) A U251-GFP tumor identified in cortical brain by EGFP fluorescence before conducting glutamate release assays. Scale bar, 1 mm. (**e**) Extracellular glutamate, released in the presence of 100 µM cystine (Cys), comparing acute cortical brain slices from sham-operated and U251-GFP-implanted mice in the presence and absence of 250 µM SAS. Error bars show means ± s.e.m. $*P < 0.05$, $**P < 0.01$.
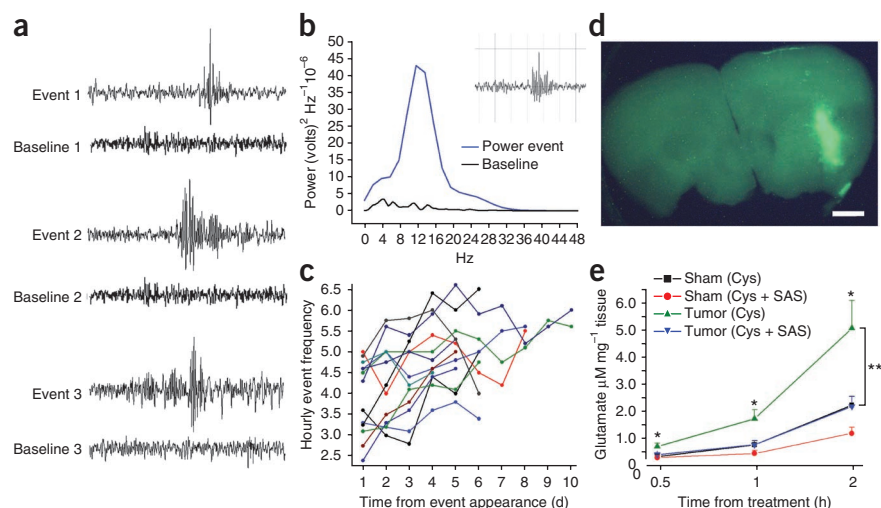
system because they retain their intrinsic gene and protein expression and invasive properties[17,18]. We initially validated tumor growth after intracranial implantation of U251 cells engineered to express firefly-luciferase (U251-ffluc) by imaging cell bioluminescence using a Xenogen IVIS system (**Supplementary Fig. 1**). In agreement with published reports[13], tumor size was similar between mice and correlated positively with bioluminescence intensity. Our histological evaluation of the resulting tumor showed invasion into the surrounding brain, as is commonly observed in the human disease (**Supplementary Fig. 2**). We validated expression of xCT, the catalytic subunit of system x_c^-, in all tumor types by western blotting, and, using ^{3}H-glutamate tracer studies, we showed functional system x_c^- activity that was SAS-sensitive and Na$^+$-independent (**Supplementary Fig. 3**).

We placed intracranial EEG electrodes in 86 glioma-implanted mice and 14 sham-operated control mice (sham) 1 week after glioma cell implantation. One week later, we conducted continuous EEG/video monitoring for 10–14 d. We observed spontaneous, recurring and unprovoked abnormal EEG activity in 37.2% of glioma-bearing mice ($n = 32$) (**Fig. 1a**). Event duration was between 0.5 and 1 s (0.538 s ± 0.113,

$n = 400$) (**Fig. 1a**), and events showed a discrete rise in the power spectrum at 12–15 Hz (**Fig. 1b**). Activity increased progressively over time (**Fig. 1c**). We detected no abnormal activity in any sham mouse. Although three mice showed epileptic activity that progressed to tonic-clonic convulsions, the behavioral phenotype typically associated with these EEG events was subtle; mice showed freezing behavior with facial automatisms and head tremor, a finding consistent with a previous study in glioma-bearing rats[7]. We found that EEG activity was similar in duration, amplitude and frequency to that described for post-traumatic epilepsy in humans and rodents[19]; thus, here we refer to this as epileptic activity[19].

Glutamate release is inhibited by blocking system x_c^-

We hypothesized that the epileptic activity in glioma-bearing mice was a result of glutamate release by the tumor via the system x_c^- transporter. We prepared acute cortical slices from seven sham mice and from nine U251-GFP–bearing mice, in which the presence of tumor was confirmed by EGFP fluorescence (**Fig. 1d**). Glutamate release into the bath was measured from individual slices (three slices per mouse) in the presence of 100 µM cystine by tandem HPLC–mass spectrometry. Glioma-bearing slices showed a time-dependent increase in glutamate compared with sham (control) slices, with concentrations increasing to 5 µM after 2 h of incubation (0.5 h: 0.3675 ± 0.07 control, 0.735 ± 0.111 tumor; 1 h: 0.7941 ± 0.15 control, 1.745 ± 0.33 tumor; 2 h: 2.242 ± 0.33 control, 5.059 ± 1.01 tumor) ($*P < 0.05$) (**Fig. 1e**). Because of glutamate dilution in the bath and astrocytic uptake in tumor-free areas, the absolute concentration within peritumoral tissue is likely to be higher. To show that glutamate release occurred through system x_c^-, we incubated an identical number of slices from the same animals in a bath containing 250 µM SAS. SAS-treated slices released significantly less glutamate (1 h: 0.7984 ± 0.15; 2 h: 2.199 ± 0.36) ($**P < 0.01$) (**Fig. 1e**). In sham slices, we found that glutamate release was unaffected by SAS, suggesting that system x_c^- does not contribute substantially to glutamate release in tumor-free brain.
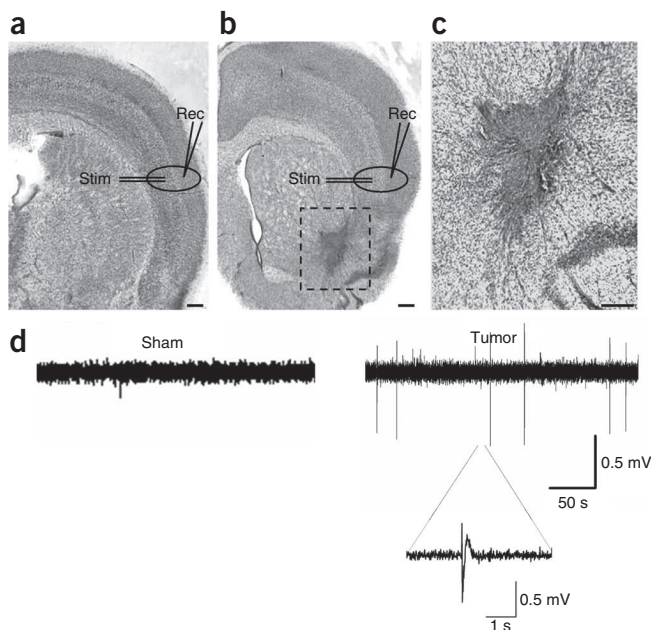

Figure 2 Acute cortical slices from tumor-bearing mice show spontaneous epileptiform activity. (**a,b**) Cresyl violet–stained brain slices from a sham (**a**) and a glioma-implanted mouse (**b**). Recording (Rec) and stimulating (Stim) electrodes were placed in peritumoral regions and in corresponding regions of sham slices as shown. Scale bars, 350 µm. (**c**) Higher-magnification image of the tumor shown in (**b**, box). Scale bar, 150 µm. (**d**) Extracellular field recordings conducted in the presence of Mg^{2+} comparing spontaneous activity in a slice from a representative U251-GFP–bearing mouse to a slice from a sham animal.

Figure 3 Acute cortical slices from tumor-bearing mice are hyperexcitable. (**a**,**b**) Whole-cell recordings from representative neurons in a cortical slice from a sham-operated (**a**) versus tumor-bearing mouse (**b**) before (ACSF) and after removal of Mg^{2+} (Mg^{2+}-free). Individual events are shown on an expanded time scale below each recording. (**c**) Mean latency to development of epileptiform activity comparing neurons from sham mice, to peritumoral neurons in animals implanted with U251-GFP, GBM12 and GBM22 tumors (*$P < 0.05$). (**d**) Mean event duration recorded in sham, U251, GBM12 and GBM22-containing brain slices. Error bars represent means ± s.e.m.
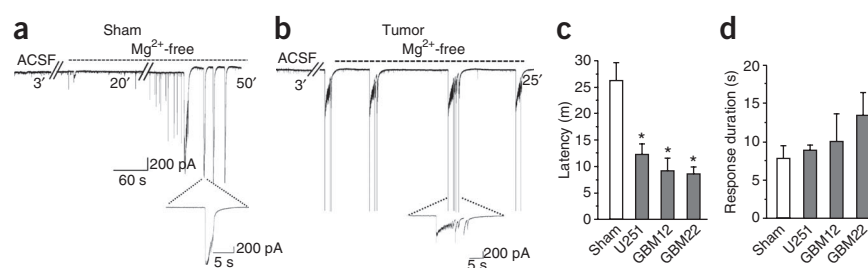
Gliomas induce spreading epileptiform activity

We next examined whether peritumoral brain shows abnormal spontaneous activity. We placed an extracellular field recording electrode in cortical layers 2 and 3, 0.5–1.5 mm from the tumor, and in comparable regions of sham cortex (**Fig. 2a–c**). We observed short spontaneous paroxysmal discharges (100–500 ms) in 23% of slices from 12 U251-GFP glioma-bearing mice in Mg^{2+}-containing artificial cerebrospinal fluid (ACSF) ($n = 43$), yet these were absent in slices from five sham mice ($n = 27$) (**Fig. 2d**). We validated slice viability by recording evoked activity in response to field electrode stimulation in deeper layer 4 (data not shown).

To further assess peritumoral neuronal excitability, we obtained whole-cell patch-clamp recordings from neurons in slices from 19 glioma-bearing and 4 sham mice. We enhanced excitability by removing extracellular Mg^{2+} that normally blocks *N*-methyl-D-aspartate (NMDA) receptors (NMDARs)[20,21]. We conducted all recordings in 100 µM cystine to ensure sufficient substrate availability for system x_c^-. Peritumoral neurons showed a significantly shorter latency to the first epileptiform discharge in slices containing U251-GFP (12 min ± 2, $n = 16$, *$P < 0.05$), GBM12 (9 min ± 2.5, $n = 7$, *$P < 0.05$) or GBM22 (8.5 min ± 1.3, $n = 13$, *$P < 0.05$) tumors (**Fig. 3a–c**) compared with sham slices (26 min ± 3.5, $n = 16$). Event duration was similar between sham slices (7 s ± 2, $n = 11$) slices containing tumors from U251-GFP (7.8 s ± 1.7, $n = 12$, $P > 0.05$), GBM12 (8.9 s ± 0.7, $n = 5$, $P > 0.05$) and GBM22 (13 s ± 3, $n = 8$, $P > 0.05$) (**Fig. 3d**).

To evaluate peritumoral cortical network hyperexcitability, we used the voltage-sensitive dye RH414 with a Neuroplex 464 diode array to visualize the spatial-temporal propagation of voltage after brief electrical stimulation, as previously described[22]. We placed the stimulating electrode in acute cortical slices within 0.5–1.5 mm of U251-GFP tumors and in comparable anatomical areas within sham slices and visualized them with pseudocolored images corresponding to the degree of membrane depolarization. Visual observation of array data revealed more a pronounced spread of depolarization in glioma-bearing slices compared with sham slices in response to 80 µA of stimulating current (**Fig. 4a**). To quantify these differences, we measured the amplitude, voltage spread, and response duration in slices from U251-GFP–implanted ($n = 4$) and sham-operated mice ($n = 4$). We found that response amplitude and duration were not significantly different in slices at 80 µA stimulation (data not shown). However, the percentage of activated diodes registering a voltage change above baseline was significantly greater in glioma-bearing slices (30.17% ± 1.95, $n = 11$) compared with sham slices (18.77% ± 1.88, $n = 8$, ***$P < 0.001$), consistent with an increased area of excitability (**Fig. 4b**).

Properties of peritumoral layer 2 and 3 pyramidal cells

Peritumoral hyperexcitability may result from alterations of intrinsic neuronal properties, such as resting membrane potential (RMP) or input resistance. However, our findings showed that RMP (~−60 mV) and input resistance, as assessed by whole-cell current-clamp recordings in visually identified layer 2 and 3 pyramidal cells (confirmed by biocytin staining), were similar between all slices from glioma-bearing animals ($n = 43$) and controls ($n = 7$) (**Fig. 4c,d**). Peritumoral neuronal input resistance from slices containing U251-GFP (150 ± 18 MΩ, $n = 60$, $P > 0.05$), GBM12 (113 ± 9 MΩ, $n = 10$, $P > 0.05$), or GBM22 (164 ± 12 MΩ, $n = 41$, $P > 0.05$) was equivalent to slices from sham-operated mice (155 ± 18 MΩ, $n = 26$, $P > 0.05$) (**Fig. 4c**). However, we found that in peritumoral neurons, the number of action potentials fired in response
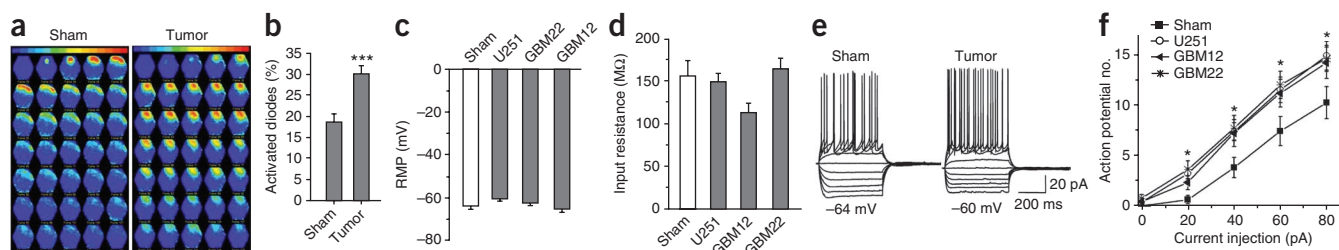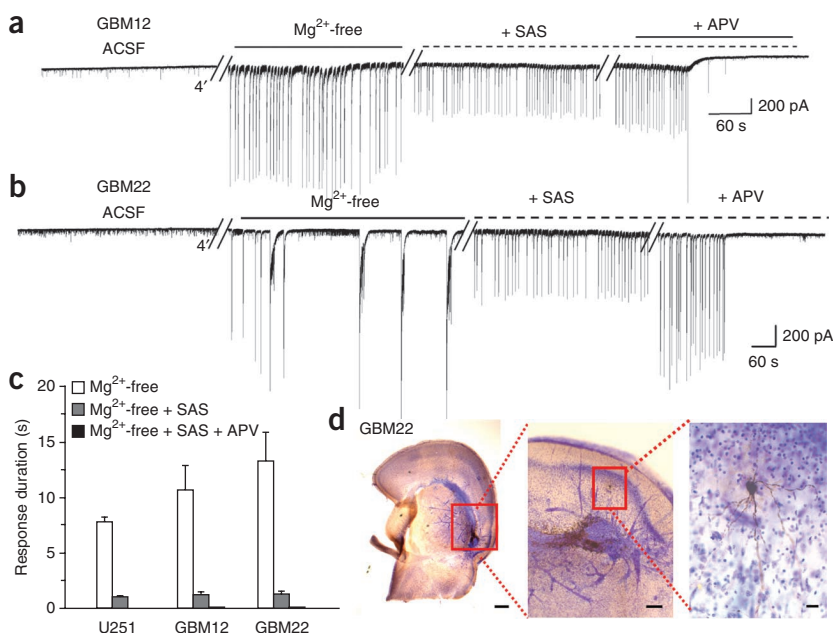

Figure 4 Cortical slices from glioma-bearing mice show increased cortical network activity and hyperexcitable layer 2 and 3 peritumoral pyramidal cells. (**a**) Representative examples of optical recordings comparing a slice from a sham and a slice from a U251-GFP–bearing mouse incubated in the voltage dye RH414 and then field stimulated with 80 µA. Each image is a pseudocolored representation of activity measured using a Neuroplex 464-diode array. Adjacent frames were recorded 1.8 ms apart. (**b**) The spread of voltage responses were measured by the number of activated diodes within the array. (**c**,**d**) Summary of RMP (**c**) and input resistance (**d**) recorded using whole-cell patch clamp in peritumoral neurons from U251-GFP, GBM12 and GBM22-implanted mice. (**e**) Examples of voltage responses to increasing amplitude current injections, from −100 pA to +80 pA (in 20-pA steps) in whole-cell current clamped pyramidal peritumoral neurons in glioma-bearing and in sham slices (pulse duration, 500 ms). (**f**) The average action potential number obtained in response to 20, 40, 60 and 80 pA depolarizing current pulses was plotted as a function of applied current yielding the input-output curves shown. Error bars show means ± s.e.m. *$P < 0.05$, ***$P < 0.01$.

Figure 5 SAS application reduces epileptiform activity in cortical slices from glioma-bearing mice. (**a**,**b**) Recordings from peritumoral neurons before (ACSF) and after removal of Mg^{2+} (Mg^{2+}-free) followed by application of SAS and APV in mice bearing GBM12 (**a**) or GBM22 (**b**) tumors. (**c**) Mean response duration for peritumoral neurons recorded in U251, GBM12 and GBM22 containing brain slices comparing recordings in Mg^{2+}-free medium to those in Mg^{2+}-free plus SAS and Mg^{2+}-free plus SAS and APV. Error bars show means ± s.e.m. (**d**) A cresyl violet–stained slice containing GBM22 shows the proximity of biocytin-filled recorded neuron (right inset, middle box) to the darker-stained tumor. Scale bars, 150 μm (left and middle); 20 μm (right inset).

to 20, 40, 60 and 80 pA current injections was significantly greater than in sham neurons (20 pA: $*P < 0.05$; 40 pA: $*P < 0.05$; 60 pA: $*P < 0.05$; 80 pA: $*P < 0.05$) (**Fig. 4e,f**), indicating a lowered excitability threshold.

Blocking system x_c^- eliminates epileptiform activity

To determine whether glutamate release from system x_c^- contributes to epileptiform activity in peritumoral brain, we obtained whole-cell patch clamp recordings from peritumoral neurons in acute brain slices from three U251-GFP ($n = 7$), three GBM12 ($n = 6$) and three GBM22 ($n = 5$) implanted mice. We observed that epileptiform activity was readily induced in Mg^{2+}-free solution in all tumor-bearing slices, as shown for representative examples of GBM12 and GBM22 peritumoral neurons (**Fig. 5a,b**). Blocking system x_c^-–mediated glutamate release with 250 μM SAS decreased the mean duration of events lasting longer than 3 s (U251-GFP: 9 ± 0.6 s; U251-GFP + SAS: 0.8 ± 0.2 s, $**P < 0.01$; GBM12: 11 ± 2 s; GBM12 + SAS: 1 ± 0.2 s, $**P < 0.01$; GBM22: 13 ± 2 s; GBM22 + SAS 1.4 ± 0.4 s, $**P < 0.01$) (**Fig. 5a–c**). The remaining events in SAS were of short duration and were reduced in amplitude to 44 ± 6% compared with the amplitude prior to drug application. All remaining activity was completely abolished after the application of 50 μM 2-amino-5-phosphonopentanoic acid (APV), an NMDA antagonist (**Fig. 5a–c**). All the peritumoral neurons we recorded were located close to tumor masses (**Fig. 5d**).

These data indicate that peritumoral neurons have a reduced excitability threshold compared to neurons from sham animals, presumably as a result of elevated levels of peritumoral glutamate. Consistent with this, bath application of 20 μM glutamate in the presence of Mg^{2+} induced epileptiform activity in 66% of U251-GFP glioma-bearing slices ($n = 9$) from four mice, but not in slices ($n = 6$) from three sham-operated mice (**Supplementary Fig. 4**). Loss of γ-aminobutyric acid (GABA)ergic inhibition may also contribute to abnormal excitability; bicuculline (BIC), a $GABA_A$ receptor antagonist, has been shown to facilitate excitatory synchronization[23]. Whole-cell recordings conducted in the presence of 10 μM BIC showed that neurons in slices ($n = 6$) from three sham mice showed typical spontaneous excitatory postsynaptic currents without development of epileptiform activity. However, spontaneous epileptiform events were observed in 50% of peritumoral neurons in 11 slices treated with BIC from three U251-GFP–implanted mice, thereby suggesting changes in both excitatory and inhibitory properties in these neurons (**Supplementary Fig. 5**).

SAS decreases epileptic activity in mice

Our biophysical data show that peritumoral epileptiform activity is inhibited by blocking system x_c^-–mediated glutamate release with SAS. If glutamate release via system x_c^- causes epileptic activity *in vivo*, we hypothesized that SAS treatment could reduce or eliminate this activity in glioma-bearing mice. Fourteen U251-GFP–implanted mice showing epileptic activity were injected intraperitoneally (i.p.) twice daily for 3 d with either 1 ml of PBS ($n = 6$) or 1 ml of 8 mg ml^{-1} SAS ($n = 8$), an equivalent dose to that typically taken by Crohn's disease patients. We analyzed EEGs recorded 4 h immediately before and 4 h immediately after treatment. We found that the frequency of activity in SAS-treated mice was significantly decreased in the 4 h after (4.25 ± 2.41) compared with the 4 h before
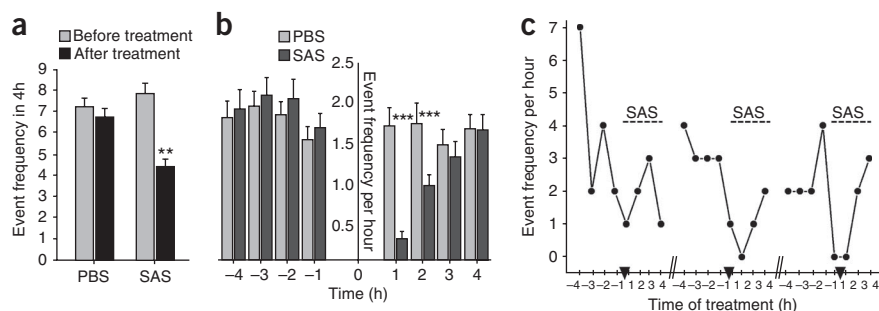

Figure 6 Sulfasalazine reduces frequency of epileptic activity in tumor-bearing mice. (**a**) The average number of epileptic events for eight SAS-treated and six PBS-treated tumor bearing mice is shown for the 4-h period before and the 4-h period after treatment. (**b**) The average hourly event frequency is plotted for eight SAS-treated mice compared with six PBS-treated mice before and after treatment. Injection time is indicated by '0'. (**c**) The number of events that occurred for each hour during the 8-h SAS treatment block (4 h before and 4 h after) is shown for one mouse; hash marks separate 3 consecutive d and arrowheads indicate the time of SAS injection. Error bars show means ± s.e.m. $**P < 0.05$; $***P < 0.01$.

treatment (7.50 ± 3.41, $**P < 0.01$) (**Fig. 6a**), but that it was unaffected by PBS treatment (before: 7.23 ± 2.09; after: 6.73 ± 2.24, $P > 0.05$). A detailed hourly analysis of treatment shows the most profound drop in frequency within the first 2 h after treatment (1h: SAS: 0.356 ± 0.091; PBS: 1.733 ± 0.22; $***P < 0.001$; 2h: SAS: 1.00 ± 0.135; PBS: 1.77 ± 0.005, $***P < 0.001$) (**Fig. 6b**). These results reflect the previously reported, relatively short biological half-life (~80 min) of SAS in the plasma of treated mice[24]. Mice did not develop a tolerance to SAS; repeated dosing showed similar efficacy suppressing epileptic activity, as shown for one representative mouse (**Fig. 6c**).

DISCUSSION

Recurring seizures, often referred to as tumor-associated epilepsy, are a well-documented yet poorly understood comorbidity affecting approximately one-third of individuals with glioma[3]. By modeling the disease in mice implanted with three different patient-derived gliomas, we show through EEG and video recording that 37.2% develop spontaneous, recurrent, abnormal EEG activity. Biophysical recordings conducted on acute cortical slices from these mice show that peritumoral neuronal hyperexcitability is attributable to glutamate release by glioma cells via the system x_c^- cystine-glutamate transporter. We measured glutamate released from glioma-bearing slices in the 5 µM range, which is sufficient to activate neuronal glutamate receptors[25], although the actual glutamate concentration to which these peritumoral neurons are exposed is likely to be much higher than what we measured in our assays because of dilution into the medium and astrocytic reuptake. A recent study done in ambulatory glioma patients measured peritumoral glutamate concentrations in excess of 100 µM (ref. 8). Peritumoral astrocytes that would normally be effective in removing and catabolizing extracellular glutamate[26] seem to be overwhelmed by glutamate release from the tumor.

Peritumoral neurons showed a lowered threshold for action potential generation and a reduced latency to development of epileptiform activity after Mg^{2+} removal compared with neurons recorded in sham-operated mice. We found that this activity was glutamate receptor–dependent and completely blocked by APV. Application of 20 µM glutamate in the presence of Mg^{2+} induced hyperexcitability in peritumoral but not sham neurons. Therefore, we suggest that the reduced activation threshold for peritumoral neurons can be largely attributed to an enhanced glutamatergic drive with a contribution of reduced GABAergic inhibition. Further studies will need to examine changes in peritumoral transmitter receptors in greater detail.

Elevated levels of extracellular glutamate have previously been implicated in development of seizures and epilepsy[27–29], although in those studies the glutamate source was neuronal. In glioma-bearing mice (our study) and rats[30], the primary glutamate source is the growing tumor. We show in mice that glutamate release by gliomas is through system x_c^- because it is Na^+-independent, cystine-dependent and blocked by SAS. Previous studies similarly show system x_c^-–mediated glutamate release from gliomas *in vitro*[9], *in situ*[31] and *in vivo*[32], leading to tumor growth[13], tumor-associated excitotoxicity[32] and edema[32,33].

We found that SAS treatment reduced epileptic activity in glioma-bearing mice, implicating glutamate release via system x_c^- in the generation of tumor-associated epileptic events. System x_c^- may also generate epileptic events in humans. Together with previous studies, our findings establish that system x_c^- is a viable new target for seizure treatments. The effects of SAS are encouraging, particularly because SAS is an FDA-approved drug with well-described, tolerable side effects that support its use as adjuvant treatment for peritumoral epilepsy. A clinical trial conducted on several end-stage glioblastoma patients with poor neurological status used SAS to inhibit nuclear factor κB; they reported no significant impact on tumor growth[34]. However, this study enrolled a severely ill, neurologically impaired patient population and did not assess antiepileptic effects[34]. Seizures often present early in disease progression and particularly affect patients with low-grade, slow-growing tumors that can become refractory to traditional antiepileptic drugs; accordingly, these patients are the most likely to benefit from SAS treatment[1]. Clearly, our findings suggest that a well-designed clinical study of SAS treatment for low-grade glioma patients is warranted.

METHODS

Methods and any associated references are available in the online version of the paper at http://www.nature.com/naturemedicine/.

Note: Supplementary information is available on the Nature Medicine website.

1. Moots, P.L. *et al.* The course of seizure disorders in patients with malignant gliomas. *Arch. Neurol.* **52**, 717–724 (1995).
2. van Breemen, M.S. *et al.* Efficacy of anti-epileptic drugs in patients with gliomas and seizures. *J. Neurol.* **256**, 1519–1526 (2009).
3. Hauser, W.A., Annegers, J.F. & Kurland, L.T. Incidence of epilepsy and unprovoked seizures in Rochester, Minnesota: 1935–1984. *Epilepsia* **34**, 453–468 (1993).
4. During, M.J. & Spencer, D.D. Extracellular hippocampal glutamate and spontaneous seizure in the conscious human brain. *Lancet* **341**, 1607–1610 (1993).
5. Patt, S. *et al.* Source localization and possible causes of interictal epileptic activity in tumor-associated epilepsy. *Neurobiol. Dis.* **7**, 260–269 (2000).
6. Senner, V. *et al.* A new neurophysiological/neuropathological *ex vivo* model localizes the origin of glioma-associated epileptogenesis in the invasion area. *Acta Neuropathol.* **107**, 1–7 (2004).
7. Köhling, R., Senner, V., Paulus, W. & Speckmann, E.J. Epileptiform activity preferentially arises outside tumor invasion zone in glioma xenotransplants. *Neurobiol. Dis.* **22**, 64–75 (2006).
8. Marcus, H.J., Carpenter, K.L., Price, S.J. & Hutchinson, P.J. *In vivo* assessment of high-grade glioma biochemistry using microdialysis: a study of energy-related molecules, growth factors and cytokines. *J. Neurooncol.* **97**, 11–23 (2010).
9. Ye, Z.C. & Sontheimer, H. Glioma cells release excitotoxic concentrations of glutamate. *Cancer Res.* **59**, 4383–4391 (1999).
10. Ye, Z.C., Rothstein, J.D. & Sontheimer, H. Compromised glutamate transport in human glioma cells: reduction- mislocalization of sodium-dependent glutamate transporters and enhanced activity of cystine-glutamate exchange. *J. Neurosci.* **19**, 10767–10777 (1999).

11. Lyons, S.A., Chung, W.J., Weaver, A.K., Ogunrinu, T. & Sontheimer, H. Autocrine glutamate signaling promotes glioma cell invasion. *Cancer Res.* **67**, 9463–9471 (2007).

12. Kim, J.Y. *et al.* Human cystine/glutamate transporter: cDNA cloning and upregulation by oxidative stress in glioma cells. *Biochim. Biophys. Acta* **1512**, 335–344 (2001).

13. Chung, W.J. *et al.* Inhibition of cystine uptake disrupts the growth of primary brain tumors. *J. Neurosci.* **25**, 7101–7110 (2005).

14. Sato, H., Tamba, M., Ishii, T. & Bannai, S. Cloning and expression of a plasma membrane cystine/glutamate exchange transporter composed of two distinct proteins. *J. Biol. Chem.* **274**, 11455–11458 (1999).

15. de Vries, N.A., Beijnen, J.H. & van Tellingen, O. High-grade glioma mouse models and their applicability for preclinical testing. *Cancer Treat. Rev.* **35**, 714–723 (2009).

16. Fomchenko, E.I. & Holland, E.C. Mouse models of brain tumors and their applications in preclinical trials. *Clin. Cancer Res.* **12**, 5288–5297 (2006).

17. Giannini, C. *et al.* Patient tumor EGFR and PDGFRA gene amplifications retained in an invasive intracranial xenograft model of glioblastoma multiforme. *Neuro-oncol.* **7**, 164–176 (2005).

18. Sarkaria, J.N. *et al.* Identification of molecular characteristics correlated with glioblastoma sensitivity to EGFR kinase inhibition through use of an intracranial xenograft test panel. *Mol. Cancer Ther.* **6**, 1167–1174 (2007).

19. D'Ambrosio, R. *et al.* Functional definition of seizure provides new insight into post-traumatic epileptogenesis. *Brain* **132**, 2805–2821 (2009).

20. Mody, I., Lambert, J.D. & Heinemann, U. Low extracellular magnesium induces epileptiform activity and spreading depression in rat hippocampal slices. *J. Neurophysiol.* **57**, 869–888 (1987).

21. Jones, R.S. Ictal epileptiform events induced by removal of extracellular magnesium in slices of entorhinal cortex are blocked by baclofen. *Exp. Neurol.* **104**, 155–161 (1989).

22. DeFazio, R.A. & Hablitz, J.J. Horizontal spread of activity in neocortical inhibitory networks. *Brain Res. Dev. Brain Res.* **157**, 83–92 (2005).

23. Gutnick, M.J., Connors, B.W. & Prince, D.A. Mechanisms of neocortical epileptogenesis *in vitro. J. Neurophysiol.* **48**, 1321–1335 (1982).

24. Zheng, W., Winter, S.M., Mayersohn, M., Bishop, J.B. & Sipes, I.G. Toxicokinetics of sulfasalazine (salicylazosulfapyridine) and its metabolites in B6C3F1 mice. *Drug Metab. Dispos.* **21**, 1091–1097 (1993).

25. Herman, M.A. & Jahr, C.E. Extracellular glutamate concentration in hippocampal slice. *J. Neurosci.* **27**, 9736–9741 (2007).

26. Danbolt, N.C. Glutamate uptake. *Prog. Neurobiol.* **65**, 1–105 (2001).

27. Rothstein, J.D. *et al.* Knockout of glutamate transporters reveals a major role for astroglial transport in excitotoxicity and clearance of glutamate. *Neuron* **16**, 675–686 (1996).

28. Meldrum, B.S. The role of glutamate in epilepsy and other CNS disorders. *Neurology* **44**, S14–S23 (1994).

29. Tanaka, K. *et al.* Epilepsy and exacerbation of brain injury in mice lacking the glutamate transporter glt-1. *Science* **276**, 1699–1702 (1997).

30. Behrens, P.F., Langemann, H., Strohschein, R., Draeger, J. & Hennig, J. Extracellular glutamate and other metabolites in and around RG2 rat glioma: an intracerebral microdialysis study. *J. Neurooncol.* **47**, 11–22 (2000).

31. Takano, T. *et al.* Glutamate release promotes growth of malignant gliomas. *Nat. Med.* **7**, 1010–1015 (2001).

32. Savaskan, N.E. *et al.* Small interfering RNA-mediated xCT silencing in gliomas inhibits neurodegeneration and alleviates brain edema. *Nat. Med.* **14**, 629–632 (2008).

33. Engelhorn, T. *et al.* Cellular characterization of the peritumoral edema zone in malignant brain tumors. *Cancer Sci.* **100**, 1856–1862 (2009).

34. Robe, P.A. *et al.* Early termination of ISRCTN45828668, a phase 1/2 prospective, randomized study of sulfasalazine for the treatment of progressing malignant gliomas in adults. *BMC Cancer* **9**, 372 (2009).

ONLINE METHODS

Glioma cells. We used the human glioma cell line U251-MG (glioblastoma multiforme (GBM), World Health Organization (WHO) grade IV) to generate U251-GFP cells. GBM12 and GBM22 tumors, previously established from human biopsies, were prepared for implantation as previously described[17,18]. All procedures were approved and carried out under the guidelines of the Institutional Animal Care and Use Committee of the University of Alabama at Birmingham.

Intracranial xenografts. We intracranially implanted either 5×10^5 U251-GFP, 2.5×10^5 GBM12 or 2.5×10^5 GBM22 glioma cells in 10 µl of 5% (wt/vol) methylcellulose stereotactically into the left hemisphere of 8–10-week-old female C.B.17 severe combined immunodeficient (SCID) mice, as previously described[35]. Control mice were injected with methylcellulose.

EEG acquisition. We placed intracranial recording electrodes (Plastics One) on the right hemisphere with a ground on the left. We acquired data (250 Hz sampling rate) using eight Biopac Systems amplifiers and AcqKnowledge 4.0 EEG Acquisition and Reader Software (Biopac Systems). Digitized files were analyzed offline by a blinded investigator using AcqKnowledge 4 software. Events of 12–15 Hz and ≥ 5× baseline amplitude were flagged for further analysis; duration, amplitude and frequency were computed in AcqKnowledge software. We used corresponding video (L20WD800 Series, Lorex Technology) to assess behavior.

Glutamate release assays. Coronal brain slices (300 µm; $n = 3$ for each experiment) were recovered for 1 h in ACSF, then transferred to 200 µl of buffer containing either 100 µM cystine or 100 µM cystine and 250 µM SAS. We removed 25-µl samples after 30, 60, and 120 min (volume maintained) for analysis at the University of Alabama at Birmingham Mass Spectrometry Core Facility using previously described tandem HPLC–mass spectrometry methods[36] with a liquid chromatography column (Waters Acquity UPLC hydrophilic interaction (ZICTM-HILIC, 20 mm × 2.1 mm, 35 µm) and 5 µm premicrofilter (The Nest Group).We quantified glutamate using the Applied Biosystems/MDS Sciex API-3200 triple quadrupole instrument in negative chemical ionization (APCI) mode, and data were acquired and analyzed using Analyst 1.4.2 software (Applied Biosystems). Results are expressed as µM glutamate per mg of wet tissue.

Electrophysiology. Anesthetized mice were decapitated and brains immersed in ice-cold ACSF (135 mM N-methyl-D-glucamine (NMDG), 1.5 mM KCl, 1.5 mM KH_2PO_4, 23 mM choline bicarbonate, 25 mM D-glucose, 0.5 mM $CaCl_2$, 3.5 mM $MgSO_4$) (Sigma-Aldrich). Coronal slices (300 µm) were recovered for 1 h in ACSF (125 mM NaCl, 3 mM KCl, 1.25 mM NaH_2PO_4, 25 mM $NaHCO_3$,

2 mM $CaCl_2$, 1.3 mM $MgSO_4$, 25 mM glucose) at 37 °C and then transferred to a recording chamber. We obtained whole-cell recordings using an Axopatch 1B amplifier (Molecular Devices) and an intracellular solution of 134 mM potassium gluconate, 1 mM KCl, 10 mM HEPES, 2 mM Mg-ATP, 0.2 mM Na-GTP and 0.5 mM ethylene glycol tetraacetic acid (EGTA) (pH 7.4, 285–290 mOsm). We made tight seals with patch electrodes (KG-33 glass, Garner Glass) with a 3–5-MΩ open-tip resistance at −70 mV. Tumors were identified by fluorescence or bright-field microscopy (**Supplementary Fig. 5**), and layer 2/3 peritumoral pyramidal cells were visualized using a Zeiss Axioscope microscope, a 40× water-immersion lens and infrared illumination. We conducted whole-cell recordings in the presence of 0.100 mM cystine. External solutions contained 0.250 mM SAS, 0.05 mM APV, 0.010 mM glutamate, 0.020 mM glutamate or 0.010 mM BIC. For extracellular recordings, coronal slices (400 µm) were recovered for 1 h at RT, placed in an interface chamber (Fine Science Tools) and superfused 1–2 ml min⁻¹ with 95% O_2 and 5% CO_2 in ACSF at 34 ± 1 °C for 1 h. We conducted field recordings using ACSF-filled glass pipettes. Data were acquired using Clampex 10 software and a Digidata 1440A interface (Molecular Devices) filtered at 5 kHz, digitized at 10–20 kHz and analyzed using Clampfit 10.0 software (Molecular Devices).

Optical recordings. We conducted optical recordings on an Axiovert 135 TV (Zeiss) microscope using a NeuroPlex 464-element photodiode array (RedShirtImaging), as previously described[22]. We placed a bipolar electrode in cortical layer 2/3 adjacent to a U251-GFP tumor, measured resting light intensity and stimulated slices at 80 µA. Signals are represented as percentage change in fluorescence ($\Delta F * F^{-1}$). We used a noise-minimizing subtraction procedure to collect data over 3 trials, and analyzed peak amplitude, signal decay and number of 3× baseline amplitude signals (spread) using custom interactive data language (IDL) programs (Research Systems).

Statistical analyses. We computed P values for biophysical recordings using unpaired two-tailed Student's t test; P values were computed for glutamate assays and mouse treatments with one-way analysis of variance (ANOVA) and Tukey-Kramer Multiple Comparisons Tests. Statistics were generated with GraphPad InStat 3.06 (GraphPad Software), significance set at $P < 0.05$, and graphed using Origin 7.5 (Microcal Software).

Additional methods. Detailed methodology is described in the **Supplementary Methods**.

35. Soroceanu, L., Gillespie, Y., Khazaeli, M.B. & Sontheimer, H. Use of chlorotoxin for targeting of primary brain tumors. *Cancer Res.* **58**, 4871–4879 (1998).
36. Buck, K., Voehringer, P. & Ferger, B. Rapid analysis of GABA and glutamate in microdialysis samples using high-performance liquid chromatography and tandem mass spectrometry. *J. Neurosci. Methods* **182**, 78–84 (2009).